stellarator news

Published by Fusion Energy Division, Oak Ridge National Laboratory
Building 5700 P.O. Box 2008 Oak Ridge, TN 37831-6169, USA

Editor: James A. Rome Issue 119 April 2009
E-Mail: jar@ornl.gov Phone (865) 482-5643
On the Web at *http://www.ornl.gov/sci/fed/stelnews*

Numerical investigation of electron orbits in the Columbia Non-neutral Torus

1. Introduction

The Columbia Non-neutral Torus (CNT) is a simple stellarator made of only four planar coils and dedicated to the study of plasmas of arbitrary neutrality confined on magnetic surfaces [1, 2]. This is not an optimized stellarator, and it exhibits large variations in magnetic field strength on surfaces. However, confinement is expected to be good because of the large radial electric field created by charge imbalance in non-neutral plasmas [3, 4].

In particular, for pure electron plasmas confined on magnetic surfaces the electric potential Φ is dictated by a Poisson-Boltzmann equation [3]:

$$\nabla^2\Phi = \frac{e}{\varepsilon_0} N(\psi)\exp\left(\frac{e\Phi}{T_e(\psi)}\right), \qquad (1)$$

where ψ is a label for magnetic surfaces, and $N(\psi)$ is a function constant on surfaces which, along with the exponential term, determines the density. The electron temperature, $T_e(\psi)$ is also constant on surfaces due to fast streaming of electrons along field lines. In CNT T_e is typically around 4 eV. A 3-D code was developed to solve Eq. (1) in the nontrivial geometry of CNT [5]. This code shows that the potential varies significantly on magnetic surfaces when there are few Debye lengths in the plasma ($a \le \lambda_D$), but tends to be constant on surfaces when many Debye length are present ($a \ge 10\lambda_D$). However, the equilibria are quite sensitive to electrostatic boundary conditions. In CNT, in the absence of the good conductor surrounding the plasma that was recently installed, and even for $\lambda_D = 1.5$ cm « $a \approx 15$ cm, potential variations on the outer surfaces are significant. This should be contrasted with quasineutral plasmas in equilibrium on magnetic surfaces in which potential variations on surfaces are essentially absent. Potential variations may only be present dynamically, and at lower values than those considered in this article, in the form of electrostatic turbulence.

Because of the electron space charge, all equilibria exhibit very strong negative electric fields ($e|\Delta\Phi|/T_e \gg 1$). The beneficial influence of a moderate ambipolar electric field on the confinement of quasi-neutral plasmas in stellarators was established long ago [6]. Here we investigate the effects of very strong electric fields on confinement. A purely radial electric field greatly improves the quality of the orbits, as expected; but because the electric field is so strong, toroidal resonances appear at moderately low values of the magnetic field, leading to unconfined orbits. In addition, potential variations on surfaces add to the complexity of the orbits and also lead to bad orbits.

In this issue . . .

2. Electron orbits

A. Boozer flux coordinates

We make use of Boozer flux coordinates (ψ, θ, φ) [7]. ψ is a radial coordinate proportional to the toroidal magnetic flux, with $\psi = \psi_b$ at the plasma boundary. θ and φ are poloidal and toroidal angles, respectively. In the (φ,θ) plane, field lines are straight with a slope $\iota(\psi)$, the rotational transform. These coordinates are derived in CNT using simple integration along the field lines, as described in Ref. [8].

Among the many advantages of using Boozer coordinates is that the drift motion depends only on the strength of the magnetic field, not on its direction. CNT has 2-fold periodicity and stellarator symmetry about the point (φ,θ) = (0,0), meaning that the magnetic field strength can be described as $B = \Sigma b_{mn} \cos(m\theta - 2n\varphi)$. The $n = 0$ components of B are the toroidal components, whereas the $n \neq 0$ components are the helical components. For an accurate description of the magnetic field we keep about 60 terms in this Fourier series. A magnetic field strength of 0.1 T is typical of CNT and is used in this article, unless otherwise stated.

B. Choice of electric potential

We will focus our attention on three different electrostatic potentials. In Section 3, we investigate the electron orbits in the absence of an electric field, $\Phi = 0$. This represents the situation where there is negligible space charge and serves to illustrate the quality of the orbits given the magnetic topology without electrostatic (primarily $\boldsymbol{E} \times \boldsymbol{B}$) effects. In Section 4, we investigate the orbits in the case of a strong electric potential, constant on the magnetic surfaces. This is an idealized situation that should lead to vastly improved confinement. In Section 5, we investigate an electrostatic potential that has significant variations on the magnetic surfaces. The potential chosen is a reasonably accurate representation of the actual electrostatic potential in CNT and gives rise to complicated drift orbits.

3. Electron orbits with no electric potential

As mentioned above, CNT has a very simple coil configuration. Thus its magnetic topology is very different from those of highly optimized stellarators such as W7X [10]. In particular, there are huge variations in B on surfaces, as shown in Fig. 1.

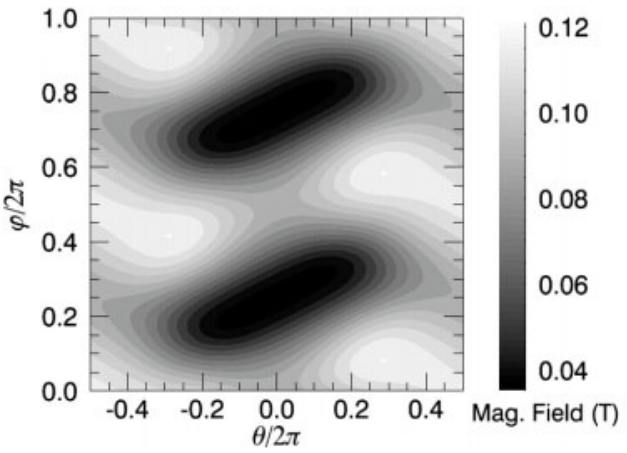

Fig. 1. Map of B on the surface $\psi = 0.5\psi_b$. One clearly distinguishes the large helical variations in B and the two troughs centered on $\theta = 0$. $\theta = 0$ corresponds to the outboard (low B region) of the torus, whereas $\theta = \pm\pi$ corresponds to the inboard (high B region) of the torus.

Because of these large variations in B there exists a very large fraction of trapped electrons, most which are helically trapped. Because these electrons are trapped in magnetic wells, they cannot take advantage of the ι-induced poloidal rotation. These trapped electrons stay localized in the poloidal direction and magnetically drift out of the torus in a time

$$t_{\text{loss}} = \frac{a}{v_D} \approx \frac{eaRB}{mv^2}, \qquad (2)$$

where a is the minor radius and R the major radius. In CNT, $a \approx 13$ cm, $R \approx 22$ cm. So for an electron with kinetic energy $W_k = 4$ eV in a $B = 0.1$ T magnetic field, this estimate yields $t_{\text{loss}} \approx 0.4$ ms. The typical orbit of a helically trapped electron is given in Fig. 2.

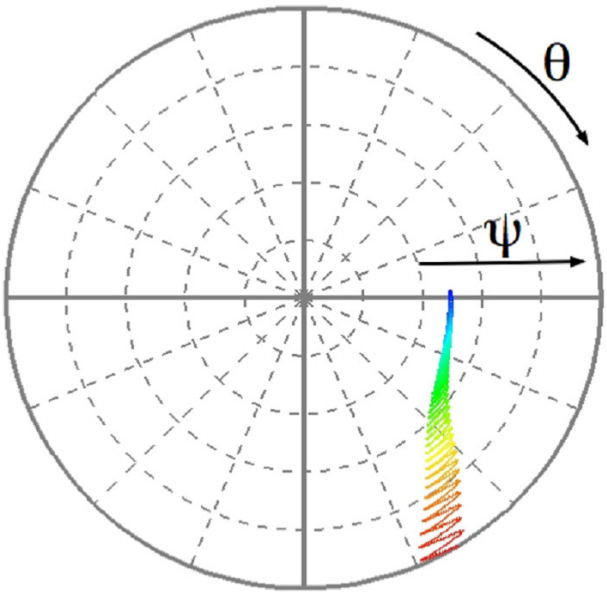

Fig. 2. Orbit of an electron in the absence of electric field. The electron, born at a minimum of B, is helically trapped and quickly lost. Color corresponds to time: blue is $t = 0$, red is $t = t_{loss}$.

Because of the large fraction of trapped electrons we expect direct losses to be large. And because all surfaces are subject to variations in B, all surfaces have a potentially large loss cone. To assess how bad the confinement of single orbits is, 1000 electrons are started on a surface and followed until they leave the confinement region, i.e., they cross the last closed flux surface. The electrons are sampled with random poloidal angle, toroidal angle, and pitch, but all have kinetic energy $W_k = 4$ eV. In Fig. 3 we plot the fraction of confined electrons as a function of time for different surfaces. We can observe that even deep in the plasma, more than half of the electrons are lost.

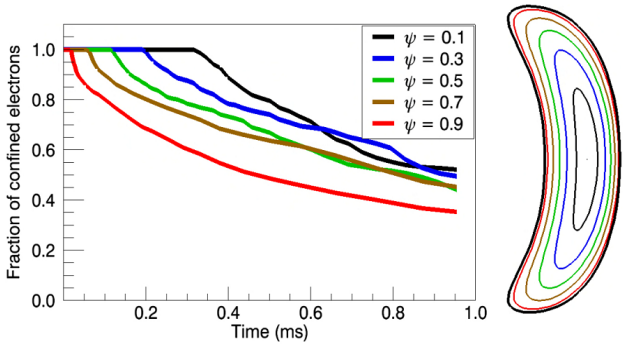

Fig. 3. Fraction of confined electrons vs time on different surfaces in the absence of electric field. 1000 4-eV electrons are initially started on each surface. At right are the corresponding surfaces seen on a cross section of the plasma.

An electron born with a pitch $\lambda = v_{||}/v$ at a location (ψ, θ, φ) is magnetically trapped on its birth surface if

$$|\lambda| \le \lambda_{max}(\psi, \theta, \varphi) \equiv \sqrt{1 - \frac{B(\psi, \theta, \varphi)}{B_{max}(\psi)}}, \qquad (3)$$

where $B_{max}(\psi)$ is the maximum of the B field on the surface ψ. However, electrons with a pitch close enough to λ_{max} are only toroidally trapped, not helically trapped. Toroidally trapped electrons, although lost in general, are lost less quickly than helically trapped electrons. This is illustrated in Fig. 4.

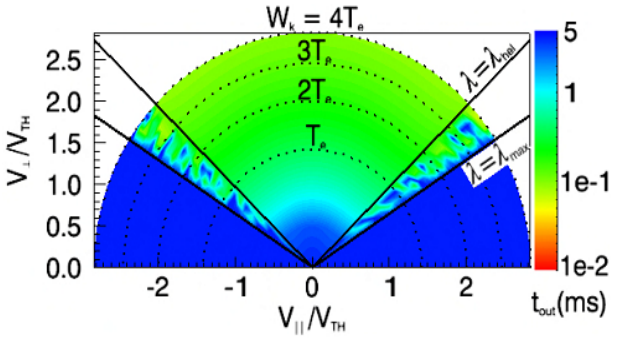

Fig. 4. Loss cone structure in the absence of electric field at a minimum of B on the surface $\psi = 0.5\psi_b$. The color (log scale) denotes the time it takes an electron to leave the confinement region. A 5-ms confinement time is considered to be infinite confinement time. One can clearly distinguish the region of helical trapping, $|\lambda| \le |\lambda_{hel}|$, from the region of toroidal trapping, $|\lambda_{hel}| \le |\lambda| \le |\lambda_{max}|$.

4. Electron orbits with electric potential constant on surfaces, $\Phi(\psi)$

A. Orbit confinement

If one adds a finite electrostatic potential that is constant on each magnetic surface, but varies from surface to surface, $\Phi = \Phi(\psi)$, this adds a purely poloidal $\boldsymbol{E} \times \boldsymbol{B}$ drift to all particles. Because the electric field is negative, this poloidal rotation is in the positive θ direction, as is the poloidal rotation induced by the rotational transform ι for forward-passing electrons. However, for ι to provide poloidal rotation, the electron must travel along the field lines, whereas the $\boldsymbol{E} \times \boldsymbol{B}$ rotation is also effective for trapped electrons. Hence the $\boldsymbol{E} \times \boldsymbol{B}$ drift can help to close the orbits of trapped electrons. As an illustration we give in Fig. 5 the orbit of the helically trapped electron in Fig. 2, this time with a strong radial electric field.

This process is effective if t_{loss}, the typical loss time of an electron, is long compared to $t_{\boldsymbol{E}\times\boldsymbol{B}}$, the half-poloidal transit time due to the $\boldsymbol{E} \times \boldsymbol{B}$ drift:

$$t_{\boldsymbol{E}\times\boldsymbol{B}} = \frac{\pi a}{v_{\boldsymbol{E}\times\boldsymbol{B}}} = \frac{\pi a^2}{\Delta\Phi}. \qquad (4)$$

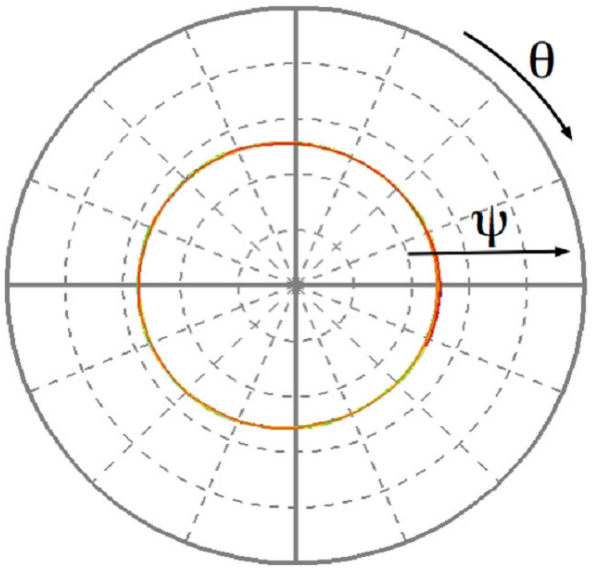

Fig. 5. Orbit of a helically trapped electron in a strong, purely radial electric field. The electron stays helically trapped but the $\boldsymbol{E} \times \boldsymbol{B}$ drift effectively closes the orbit in the poloidal direction.

As mentioned earlier, in CNT $e\Delta\Phi \gg T_e$ so that for a thermal electron

$$\frac{t_{\boldsymbol{E}\times\boldsymbol{B}}}{t_{\text{loss}}} = \frac{2\pi a}{R}\frac{W_{\text{k}}}{e\Delta\Phi} \ll 1\,, \qquad (5)$$

and closing of the orbits through $\boldsymbol{E} \times \boldsymbol{B}$ drift is very effective. This is illustrated in Fig. 6 where we plot the loss cone at a minimum of B on the surface $\psi = 0.5\psi_{\text{b}}$.

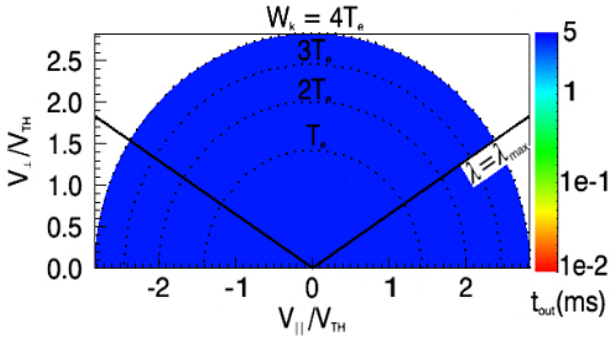

Fig. 6. Loss cone structure in the case of a strong, purely radial electric field at a minimum of B on the surface $\psi = 0.5\psi_{\text{b}}$. The color (log scale) denotes the time it takes an electron to leave confinement. A 5-ms confinement time is considered to be infinite. All trapped electrons are perfectly confined by the $\boldsymbol{E} \times \boldsymbol{B}$ rotation (compare with Fig. 4).

B. Direct losses

Only electrons that have enough kinetic energy and are born close enough to the plasma boundary can escape confinement before closing their orbits in the poloidal direction. This is confirmed numerically by running a simulation similar to the one presented in the previous section, where we start 1000 4-eV electrons on different ψ surfaces and keep track of the fraction of confined electrons in time. The initial sampling is as described before. Results are presented in Fig. 7, showing that on the $\psi = 0.5$ surface all particles are confined. In the edge region, there are some losses of energetic particles; see Fig. 8, which shows the loss cone for particles starting on the $\psi = 0.9$ surface, near the plasma edge. The loss cone in this case is somewhat similar to that without an electric potential, but now significant kinetic energy is needed even for the deeply trapped particles before they can escape.

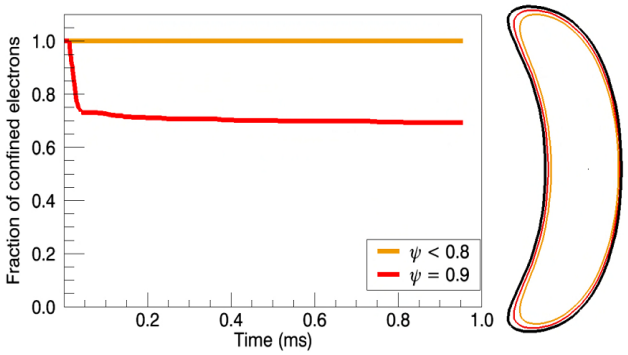

Fig. 7. Fraction of confined electrons vs time on different surfaces in the case of a strong and purely radial electric field. 1000 4-eV electrons are initially started on each surface. Only electrons born very close to the last closed surface are lost.

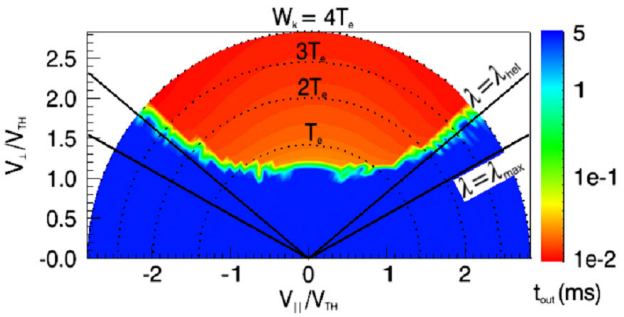

Fig. 8. Loss cone structure in the case of a strong, purely radial electric field at a minimum of B on the surface $\psi = 0.9\psi_{\text{b}}$. The color (log scale) denotes the time it takes an electron to leave confinement. A 5-ms confinement time is considered to be infinite. Only high-energy helically trapped electrons are lost.

C. Resonances

Because $\boldsymbol{E} \times \boldsymbol{B}$ rotation is in the positive θ direction, this rotation adds to the ι-induced poloidal rotation for co-passing electrons ($\lambda > 0$), whereas it subtracts from the ι-induced poloidal rotation for counter-passing electrons ($\lambda < 0$). For very strong electric fields, these two rotations can cancel out for counter-passing particles, leading to a toroidal resonance [11]. The $\boldsymbol{E} \times \boldsymbol{B}$ velocity is

$$v_{\boldsymbol{E}\times\boldsymbol{B}} = \frac{E}{B} \approx \frac{\Delta\Phi}{aB} \tag{6}$$

and the ι-induced velocity is

$$v_\iota = v_\parallel \frac{B_\theta}{B} \approx \varepsilon \iota v_\parallel , \tag{7}$$

where ε is the inverse aspect ratio $\varepsilon \equiv a/R$. Estimating ΔΦ with Poisson's equation and $v_\parallel \approx v_{th} \equiv \sqrt{T/m}$ yields the resonance condition:

$$N_D^2 \rho_L \approx \iota \varepsilon a , \tag{8}$$

where $N_D = a/\lambda_D$ is the number of Debye lengths in the plasmas and ρ_L is the electron Larmor radius. The resonance condition can be fulfilled for typical conditions of operation in CNT. For the potential we have chosen here, a resonance is observed with $B \sim 0.02$ T, which is a typical magnetic field in CNT.

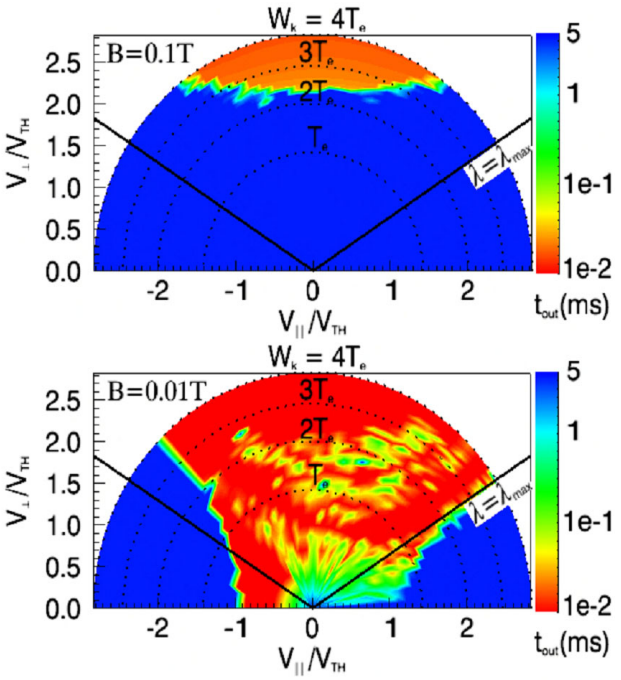

Fig. 9. Deterioration of the loss cone resulting from resonant electrons in the case of a strong and purely radial electric field. Both plots are at the same location at a minimum of B on the surface $\psi = 0.7\psi_b$. Top: $B = 0.1$ T and is far from resonance, bottom: resonances with $B = 0.01$ T.

Resonances degrade confinement because the resonant particles do not rotate poloidally, see Fig. 9.

Because of the resonance, counter-passing electron orbits are changed to banana-like orbits, see Fig. 10. These are understood as follows. In low B regions the positive $\boldsymbol{E} \times \boldsymbol{B}$ drift overcomes the negative ι-induced rotation and the net motion is in the positive θ direction. But as the electron explores the surface along the field lines, it goes to regions of higher B, which reduces the $\boldsymbol{E} \times \boldsymbol{B}$ drift. The parallel velocity, however, does not decrease appreciably because electrons subject to such effects have very small magnetic moments. This leads to a net negative θ motion. Averaged over a toroidal period, the electron experiences a slow poloidal motion in one direction. Because of this slow poloidal motion the radial drifts accumulate and the electron moves radially out (in) consequently gaining (losing) kinetic energy. At some point the kinetic energy is large (small) enough to reverse this toroidally averaged poloidal motion and the electron closes its banana-like orbit. The width of these banana orbits is very large, and electrons can be lost if the orbits intersect with the plasma boundary.

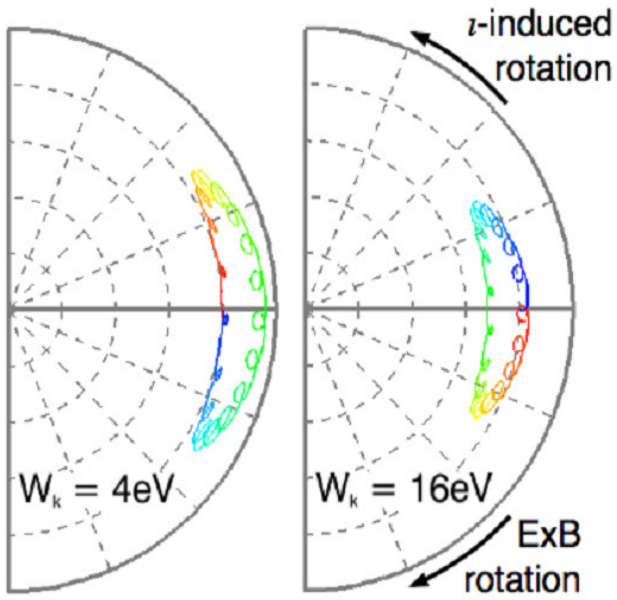

Fig. 10. Two "banana-like" orbits starting at the same initial location and with the same initial pitch ($\lambda = -1$). The only difference is the initial kinetic energy: 4 eV (left) and 16 eV (right). Color denotes time.

We must emphasize the fact that although they look similar, these banana-like orbits are very different from the ones found in tokamaks. In tokamaks, banana orbits are due to toroidicity and the direction of the shift from the flux surface depends on the sign of the initial parallel velocity of the particle. Here banana-like orbits are due to

resonances in the poloidal motion, and occur for counter-passing electrons only; the direction of the shift depends on the initial parallel kinetic energy of the electron. If the electron is born with little parallel kinetic energy, its initial poloidal motion is in the positive θ direction, whereas if it is born with a lot of parallel kinetic energy, its initial poloidal motion is in the negative θ direction.

5. Electron orbits with potential nonconstant on surfaces

We now turn to the most complicated case of an electrostatic potential depending on all three space coordinates, as is the case in CNT. Although potential variations on surfaces are essentially absent in quasineutral plasmas in equilibrium, they are inherent to non-neutral plasmas in equilibrium on magnetic surfaces. In quasineutral plasmas, potential variations may be present dynamically and at lower values in the form of electrostatic turbulence.

Variations in the electric potential in the poloidal direction create radial $\boldsymbol{E} \times \boldsymbol{B}$ drift. This drift does not depend on the kinetic energy of the electron as magnetic drifts do. Even low-energy electrons can make significant radial excursions. And by doing so they can pick up kinetic energy from the electric field and effectively increase their magnetic drifts.

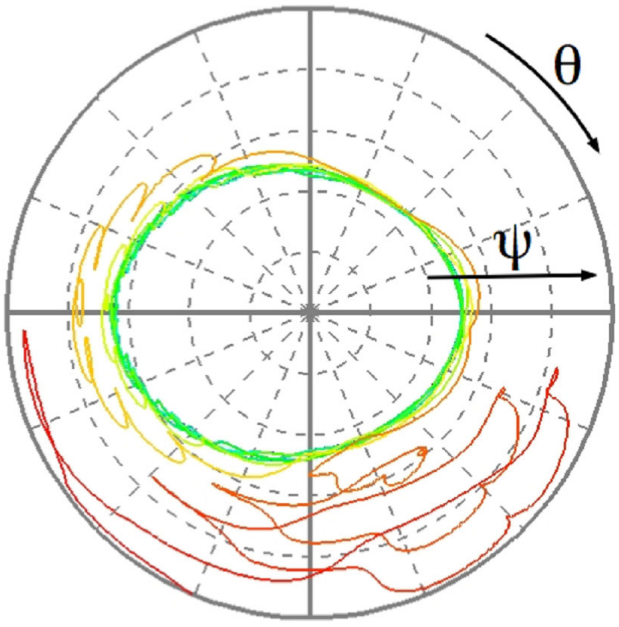

Fig. 11. Complicated orbit of an electron in the real potential of CNT, non-constant on magnetic surfaces. The electron born at $\psi = 0.5\psi_b$ with $W_k = 4$ eV ends up being lost. Color corresponds to time: blue is $t = 0$, red is $t = t_{out}$.

The combination of all these effects makes analytical calculation impractical. The complexity of the orbits is illustrated in Fig. 11, where we plot the trajectory of the same electron as in Fig. 2 and Fig. 5 but in a potential $\Phi(\psi, \theta, \varphi)$ typical of CNT before the installation of conducting boundaries.

Numerical integration of the orbits of 4-eV electrons started on different surfaces shows that there exists a large fraction of unconfined orbits exists even deep inside the plasma (see Fig. 12).

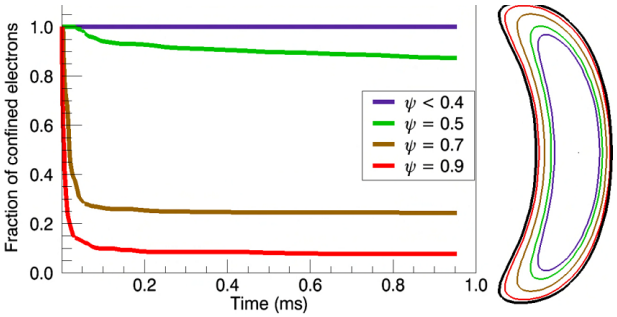

Fig. 12. Fraction of confined electrons in the case of an electric potential with significant variations on surfaces. 1000 4-eV electrons are started on each surface. Losses are significant even deep in the plasma.

Intuitively this is understood as follows. Without electric field and neglecting magnetic drifts, electrons circulate all around magnetic surfaces following field lines. Now if there is an electric field, electrons also experience $\boldsymbol{E} \times \boldsymbol{B}$ drift on equipotential surfaces because $v_{\boldsymbol{E}\times\boldsymbol{B}} = \boldsymbol{E} \times \boldsymbol{B}/B^2 = -\nabla\Phi \times \boldsymbol{B}/B^2$, so that $v_{\boldsymbol{E}\times\boldsymbol{B}} \cdot \nabla\Phi = 0$. And if the equipotential surfaces do not match magnetic surfaces, electrons can undergo $\boldsymbol{E} \times \boldsymbol{B}$ drift from one magnetic surface to another. After a few steps of jumping from one surface to the other an electron can find its way out of the plasma (see Fig. 13). Simulations show that this process is quite effective and can remove electrons from the plasma in tenths of microseconds (see Fig. 12).

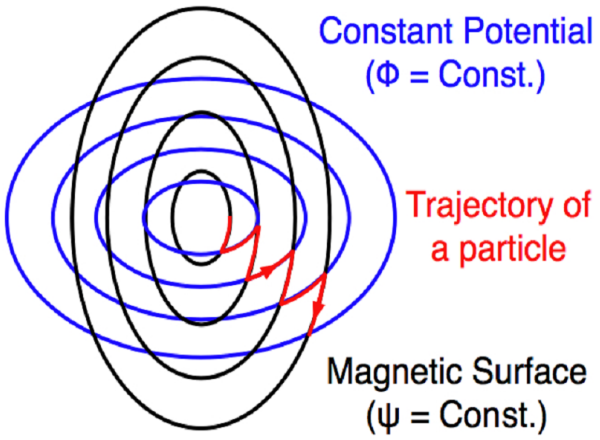

Fig. 13. Conceptual sketch of an orbit when there is a mismatch between equipotentials and magnetic surfaces. Electrons jump from magnetic surface to magnetic surface by drifting on equipotentials and can find their way out of the plasma.

6. Conclusion

The strong radial electric field created by charge imbalance in CNT has been shown to greatly improve the orbits, as expected. However, two main mechanisms have been identified that can create bad orbits in CNT despite this large radial electric field. First, even when the electric potential is perfectly constant on surfaces, toroidal resonances occurring at low magnetic field B that destroy orbit confinement. Second, nonconstancy of the electric potential on surfaces also creates bad orbits. The electric potential used in Section 5 is the potential in CNT with electrostatic boundary conditions imposed by the coils and the vacuum chamber. The recent installation of a conducting boundary surrounding the plasma should then considerably improve the orbits. Indeed, even if this does not make the potential perfectly constant on surfaces, it certainly greatly reduces the variations on surfaces. Experimental and numerical work is currently being carried out to characterize more precisely how the potential at the plasma boundary is affecting the orbits and transport in CNT.

Acknowledgments

This work is supported by the National Science Foundation-Department of Energy Partnership in Basic Plasma Science under Grant NSF-PHY-06-13662.

Benoit Durand de Gevigney, Thomas Sunn Pedersen,
and Allen H. Boozer
Applied Physics and Applied Mathematics Department
Columbia University, New York, New York 10027

References

[1] T. Sunn Pedersen, A. H. Boozer, J. P. Kremer, R. G. Lefrancois, W. T. Reiersen, F. Dahlgren, and N. Pomphrey, Fusion Sci. Technol. **46**, 200 (2004).

[2] T. Sunn Pedersen, J. P. Kremer, R. G. Lefrancois, Q. R. Marksteiner, N. Pomphrey, W. T. Reiersen, F. Dahlgren, and X. Sarasola, Fusion Sci. Technol. **50**, 372 (2006).

[3] T. Sunn Pedersen, Phys. Rev. Lett. **88**, 205002 (2002).

[4] J. W. Berkery and A. H. Boozer, Phys. Plasmas **14**, 104503 (2007).

[5] R. G. Lefrancois, T. Sunn Pedersen, A. H. Boozer, and J. P. Kremer, Phys. Plasmas **12**, 072105 (2005).

[6] H. E. Mynick, Phys. Fluids **26**, 2609 (1983).

[7] A. H. Boozer, Phys. Fluids **24**, 1999 (1981).

[8] G. Kuo-Petravic and A. H. Boozer, J. Comput. Phys. **51**, 261 (1983).

[9] A. H. Boozer and G. Kuo-Petravic, Phys. Fluids **24**,851 (1981).

[10] G. Grieger, W. Lotz, P. Merkel, J. Nührenberg, J. Sapper, E. Strumberger, H. Wobig, the W7-X Team, R. Burhenn, V. Erckmann, et al., Phys. Fluids B **4**, 2081 (1992).

[11] U. Stroth, Transport in Toroidal Plasmas, vol. 670 of Lecture Notes in Physics (Springer Berlin / Heidelberg, 2005).

[12] J. Fajans, Phys. Plasmas **10**, 1209 (2003).

Motojima succeeded by Komori at NIFS

Professor Akio Komori was appointed to be the next Director-General of the National Institute for Fusion Science (NIFS) as the successor of Professor Osamu Motojima, who completed his term of six years on March 31, 2009.

Professor Komori earned a Ph.D. in nuclear fusion science, plasma physics, at Tohoku University in 1978, and performed research at Oak Ridge National Laboratory, Tohoku University, and Kyushu University. He has worked at NIFS since 1993, and has been the Director of the Department of Large Helical Device Project since 2003.

His term of office as the Director-General will be 4 years, from April 1, 2009 to March 31, 2013.

http://www.nifs.ac.jp/en/press/081218.html